Article

Not peer-reviewed version

Myth and True Identity of Dark Energy

Antonio Codino *

Posted Date: 25 February 2026

doi: 10.20944/preprints202602.1430.v1

Keywords: electrostatic fields in galaxy clusters; Dark Energy; expansion of the universe; acceleration of universe; dark matter in galaxy clusters

 doi:10.20944/preprints202602.1430.v1

Article

Myth and True Identity of Dark Energy

Antonio Codino

Scientific associate of *INFN*, Italy; antonio.codino@pg.infn.it

Abstract

Dark Energy entered the arena of the speculative physics since 30 years after the observation of the slight acceleration of material bodies established by supernovae used as standard candles in the Gigaparsec distance range. Recent advances in the study of cosmic rays redundantly indicate that galaxy clusters have permanent, steady electrostatic fields of maximum strength of 5 V/m, general centripetal direction and electrostatic potentials 10^{21}-10^{23} $Volt$. This work determines for the first time how the slight acceleration of material bodies, in the interval 10^{-10}- 10^{-13} m/s^2, is caused by electrostatic fields in galaxy clusters and that Dark Energy is electrostatic energy. Unlike matter that is concentrated in galaxies and galaxy clusters, electrostatic energy at cosmic scale is quite diffuse. Empirical evidence of the electrostatic fields is based on the rich and variegated synchrotron emission in galaxy clusters and, notably, on the absence of diffuse gamma rays in galaxy clusters which amounts to three orders of magnitude relative to current, reiterated predictions and on other data.

Keywords: electrostatic fields in galaxy clusters; Dark Energy; expansion of the universe; acceleration of universe; dark matter in galaxy clusters

---

1. Introduction

The concept of *Energy* was invented in the last four centuries. The concept reached its climax in *Thermodynamics* where a precise nexus between heat content of material bodies and the motion of their internal constituents was established in 1900. Subatomic and subnuclear particles down to sizes of 10^{-18} *meters* benefit and have immensely benefited of the energy concept via *Quantum Mechanics*.

By more than a century, it is also known, that spiral nebulae or galaxies around the Earth have receding velocities ; in 1917 Melvin Vesto Slipher reported 22 receding galaxies and 3 approaching in a sample of 25 measured redshifts [1]. At a distance of about 10^{26} *meters* galaxies incredibly graze the natural velocity limit of 299 792 km/s or 29.97 cm/ns. Moreover, observational astronomy reported in 1998 [2,3] that beyond distances of about 500 Mpc from the Earth, galaxies slightly accelerate; they do not decelerate as gravity force encapsulated in any theoretical model would dictate. From this acceleration budded the term *Dark Energy* but not the more realistic and appropriate *Dark Acceleration* ; dark because unexplained, unexpected, in the penumbra of Physics.

This study intends to prove that the slight acceleration of galaxies beyond and around 1 Gpc is imparted by the electrostatic fields in galaxy clusters. Electrostatic fields in galaxy clusters are generated by cosmic rays and they were first introduced in 2021 [4] and amply justified in the oversize research document published in 2022 [5].

The essential result of this paper is anticipated here : *Dark Energy* is the energy of electrostatic fields in galaxy clusters which repels and overwhelms gravity attraction in the time lapse of a few billion years from an initial condition identified by the measured properties of the cosmic microwave radiation. The empirical evidence of the electrostatic fields in galaxy clusters is multifaceted [5]. The absence of diffuse gamma rays in galaxy clusters [6,7] attested by all experiments since the EGRET scrutiny [8] represents a direct proof of the presence of negative charge in galaxy clusters.

As gravity compresses the interdistances of the material bodies, exacting deceleration, the reported acceleration [2,3] demonstrates that any theoretical models based only on gravity attraction are

 doi:10.20944/preprints202602.1430.v1

fallacious in multiple aspects. Accordingly, this study has to necessarily define the novel context of the cosmic matter based on facts and free from stratified, specious prejudice. The *Cold Universe* attested by the temperature of the cosmic microwave radiation of 2.725 *absolute degrees* is introduced and justified in *Sec*. 2. The long time interval of the existence of the *Cold Universe* is called *Hibernation Era* which precedes the *Electrostatic Era*, the present epoch, featured by the ignition of stars and the concomitant presence of cosmic rays.

In *Section* 3 a model of electrostatic fields in rich galaxy clusters is introduced and justified. Adopting this model the electrostatic repulsion among galaxy clusters becomes quantitatively feasible. The calculation of receding velocities of galaxy clusters proceeds by two steps (*Sections* 4 and 5). The first step, which has also a pedagogical stock, is extremely useful as it bridges previous results [4] with novel results (*Section* 5). It uses a linear chain of galaxy clusters (termed here filiform chain) separated by 60 Mpc (see Figure 4) and a total linear size of 3960 Mpc, 1.22×10^{26} m.

The second step uses a three dimensional array of cubic form of galaxy clusters with the inter-distance of 60 Mpc. The acceleration of galaxy clusters versus time is discussed and elucidated both for the filiform chain and for the cubic array. Whatever are the natural limits of the parameters of the calculation, it turns out that galaxy clusters recede one another and they recede with repulsive accelerations in the range 10^{-9}-10^{-11} m/s^2 (see Figure 5) depending on cluster age and distance from the central clusters.

Conclusions and context are in *Section* 6 : *Dark Energy* is electrostatic energy. Elementary particles (for examples, *chamaleons*, *dilatons*, *tachyons*, *symmetrons*, *axions*, *gravitons* and others) postulated to constitute *Dark Energy* have never been discovered and, the simplest conclusion, is that they do not exist; they are just mathematical entities, phantoms, outside the domain of *Experimental Physics*.

As the prerequisites of this work are incompatible with the current ideas of the *universe*, some themes need a clarification. A first example : the Universe age of 13.8 billion years (hereafter *Ga* for Giga annum) is regarded as too short face to the ages of closed globular clusters [9–12] and other data [13]. A second example: the assumption of the predominant cosmology that all the material bodies were concentrated, 13.8 *Ga* ago, in a small volume or a spatial point, the *primeval atom* or the *primeval fireball* or the *cosmic egg* [14], is also regarded as an unphysical assumption, incompatible with the *First Law of Thermodynamics* and *Nuclear Physics* data (see *Appendix* A) established in accelerator experiments.

The scientific context of this work face to current ideas of the universe is further ascertained in the *Appendix* A and B.

2. The Hibernation Era at Temperature of 2.7 Degrees

An almost model independent estimate of cosmic matter around the Earth [15] indicate an approximate mass of 10^{50}-10^{52} kg disseminated over the gigantic stretch of $(0.94 - 7.3) \times 10^{26}$ m. These two data, mass and size, refer to the *observed universe* or the *nearby universe* or the *giant material bodies around the Earth* or, eventually, the *local clod* (see ref. [5], *Segment* 8.2).

Cosmic rays do exist in the Milky Way galaxy, other nearby spiral galaxies and, also, in other types of galaxies. The correlation of gamma rays versus radio continuum emission [16] and that of gamma rays versus infrared emission [17] demonstrate that cosmic rays also reside in elliptical and irregular galaxies.

 doi:10.20944/preprints202602.1430.v1

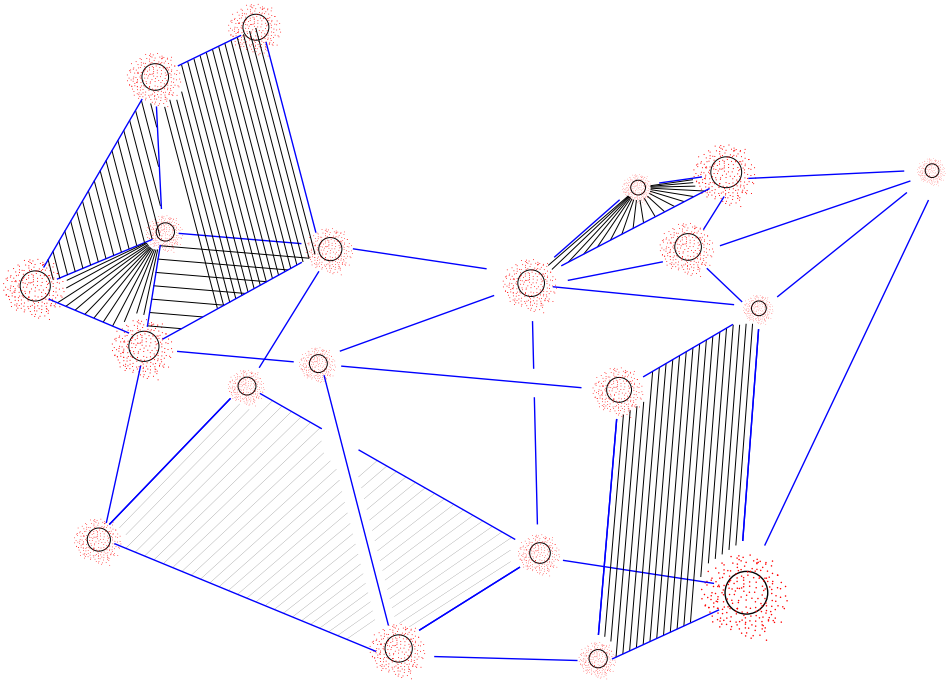

Figure 1. Artistic but essential representation of N galaxy clusters (black circles, N = 20 is arbitrary) surrounded by halos of positive electric charge of cosmic rays (red dots) with typical sizes S_c. As in this fictive view distances between any two clusters d_{nk} are much larger than the radii S_c, no significant repulsive forces is acting (n and $k \leq N$). Under this condition at the generic time interval t, the sum of the negative charge Q_{gc}^{-} retained by the *n-th* cluster with the positive charge of the cosmic nuclei Q_{gc} is zero, namely, Q_{gc}^{-} = -Q_{gc}. The condition of zero electric charge within a given volume encircling a generic cluster exactly defines the preelectrostatic epoch of the cosmic matter when only gravity forges the global dynamic status of the *local universe*. Note that the dashed parallel blue lines only intend to sketch a three dimensional image of the drawing without any other purposes. This figure reiterates in a three dimensional view the same condition limited only to a pair of galaxy clusters of fig. 1 in ref. [4].

Eruptions and explosions of the first stars of the *nearby universe* likely triggered the first populations of cosmic rays. This assertion is anchored to the fact that star formation rates are correlated with non thermal synchrotron emission (see for example, [18]) which is emitted by the cosmic-ray electrons. From the electron-to-proton flux ratios of cosmic rays in various galaxies, believed to be a variable parameter although a universal parameter, would follow the existence of cosmic-ray nuclei.

As cosmic rays pervade the peripheral volume of galaxies, whenever galaxy pairs interact in galaxy clusters, cosmic rays disseminate in the entire cluster volume. Cosmic rays, due to their dominant positive charge Q_{gc} (gc for galaxy clusters) and the their extremely high energies, also evade from the volumes of galaxy clusters populating intercluster space. As a consequence, the negative charge Q_{gc}^{-} = -Q_{gc} (made of both quiescent and cosmic-ray electrons) remains trapped in cluster volumes. It is this negative charge Q_{gc}^{-} that causes the electrostatic repulsion among clusters.

As the electrostatic repulsion determines the increase of the mutual distances of galaxy clusters [4,5] (termed in the literature and here the expansion and acceleration of the *nearby universe*), the time lapse where this repulsive effect dominates over the attractive gravity has been called *Electrostatic Era* [4,5].

 doi:10.20944/preprints202602.1430.v1

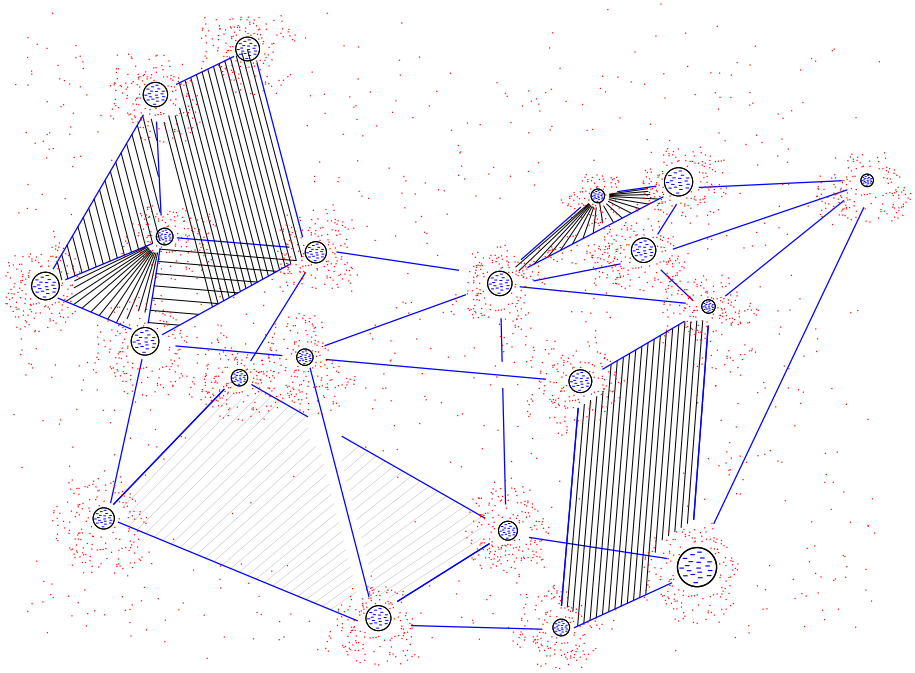

Figure 2. Illustrative scheme of the dissemination of cosmic nuclei outside galaxy clusters. Cosmic nuclei are represented by red tiny dots and they mostly reside outside cluster volumes. Cosmic nuclei inside cluster volume have been omitted to simplify the drawing. Quiescent and cosmic electrons (negative blue signs within black circles) mostly reside inside cluster volumes (black circles). By contrast with the condition expressed in Figure 1, where cosmic nuclei are always confined within the nominal intercluster distance $d_c/2 = 30\ Mpc$, here a fraction of cosmic nuclei lies beyond $d_c/2$. The negative charges within cluster volumes exert the repulsion among clusters.

The time preceding the *Electrostatic Era* is referred here to as *Hibernation Era* because the *nearby universe* is governed by gravity of the cold Hydrogen without any electric fields. The chief experimental evidence of the *Hibernation Era* is the cosmic microwave radiation with its black body spectrum centered at $6.61 \times 10^{-4}\ eV$ corresponding to a temperature of 2.725 degrees[1] discovered in 1957 [19], rediscovered in 1965 and redundantly probed by precision measurements of its properties up to the present days.

A second notable fact attesting the cold universe at the beginning of the *Electrostatic Era* (20-25 *Gy* back in time) is the increasing fraction of cold molecular Hydrogen versus lookback times up to 10 *Ga* ($\sim z = 1.5$) measured by infrared detectors [20]. Molecular Hydrogen has been detected in host galaxies of quasars with redshifts $z \geq 6$ [21] and galaxy clusters [22]. Molecular Hydrogen means low temperatures 10-30 degrees at lookback times 10-13 *Ga* and not temperatures of billion degrees.

The *EDGE* experiment located in western Australia detects the 21 cm line emitted by the neutral hydrogen with high redshift, $z \sim 17$. The observed temperature of 3.8 *degrees* [23] is below that predicted by the standard cosmology. This recent finding is again inconsistent with the *primeval fireball* at temperature of billion *degrees* but in the correct avenue of a *cold universe* at 2.725 *degrees*.

A fourth notable empirical fact attesting the *Hibernation Era* is based on the chemical evolution of matter processed by stars [24]: " Carbon is mostly produced in AGB stars and planetary nebulae most of which evolve on long timescales. Although the first AGB stars appear as soon as $\sim 50\ Myr$, after the onset of star formation, the bulk of Carbon production appears after 1 *Gyr*, yielding a delayed enrichment with respect to α-elements (e. g. Oxygen) that are promptly produced by SNII. At $z > 6$ the age of the universe is less than 1 *Gyr*, hence stellar evolution may fall short of the time needed to produce the observed large Carbon abundance ".

[1] The chief datum of the cosmic microwave radiation has been kidnapped, distorted and mystified by the doctrine of the primeval atom, a catastrophic idea with intuitive and theoretical tentacles which pervades the literature since 1927 [14] imposing enormous high temperatures of billion degrees at lookback times of 13-14 *Ga* instead of the observed temperature of 2.7 degrees

 doi:10.20944/preprints202602.1430.v1

This is the Carbon problem which indicates that the *universe* age of the dominant unreal cosmology of 13.8 *Ga* is not long enough. Thus, the extra time necessary to produce the observed Carbon abundance resonates with the globular cluster ages [9–12]. But stars blossom from cold molecular Hydrogen at temperature of 10-30 *degrees* which attests a *cold universe*.

3. Permanent Electrostatic Fields in Rich Galaxy Clusters

Galaxy clusters are moving away from each other by electrostatic repulsion [4,5]. The repulsion is caused by permanent electric fields in galaxy clusters. These fields can be described by the simple electrostatic structure termed double concentric sphere with zero charge adopted in other studies [25,26] and also applicable to spheroidal galaxies [25,26]. Electric fields in galaxy clusters are described in this work by five parameters : the mass M_c, the size defined by the radius r_c, average cluster interdistance d_c, the average propagation length of cosmic rays through the intercluster space R_c and the positive electric charge Q_{gc} = - Q_{gc}^-.

The adopted parameters are : $M_c = 2 \times 10^{47}$ g, $r_c = 2$ Mpc, $d_c = 60$ Mpc, $R_c = 150$ Mpc, and $Q_{gc} = 5.17 \times 10^{36}$ C. The positive electric charge Q_{gc} is defined by the dimensionless parameter $\zeta_c \equiv Q_{gc}/{q_b}^2$ and $q_b \equiv M_c\ (4\pi\ \epsilon_0\ G)^{1/2}$ where $\epsilon_0 = 8.85 \times 10^{-12}$ F/m and G= 6.67 42 86 $\times 10^{-11}$ m^3/s^2 kg. Thus, Q_{gc} = ζ_c $M_c\ (4\pi\ \epsilon_0\ G)^{1/2}$ = M_c 0.8617 $\times 10^{-11}$ = 5.17×10^{36} C.

It is widely known that cosmic ray density, ρ, decreases as the distance from the source increases. Accordingly the charge density ρ decreases from the cluster center. Other studies [24] justify, $\rho = k/r$ where $k = Q_{gc}^+/2\pi R_c^2$ and the related electric field, $E_+(r)$ is constant with intensity, $E_+(r) = k/2\ \epsilon_0 = Q_{gc}\ /\ (4\ \pi\epsilon_0\ R_c^2)$.

The negative electric charge, Q_{gc}^-, having spherical symmetry of diameter $2r_c$, in a generic point r in the interval $r_c < r < R_c$, has the notorious intensity, $E_-(r) = Q_{gc}^-/\ (4\pi\epsilon_0\ r^2)$. The resulting electric field, $E(r) = E_-(r) + E_+(r)$ is:

$$E(r) = E_-(r) + E_+(r) = \frac{-Q_{gc}}{4\pi\epsilon_0}(\frac{1}{r^2} - \frac{1}{R_c^2}) \tag{1}$$

where $\epsilon_0 = 8.8541 \times 10^{-12}$ F/m. Because of the postulated spherical symmetries of the positive and negative charge distributions and the common origin Ω, the electric field $\vec{E}\ (r)$ vanishes beyond the distance $R_c = 150$ Mpc.

Inside the cluster, $0 \leq r \leq r_c$, the field intensity E_- is: $-rQ_{rc}/\ 4\ \pi\epsilon_0\ r_c^3$ [25]. Accordingly, the total field $E(r)$ is :

$$E(r) = E_-(r) + E_+(r) = \frac{Q_{gc}}{4\pi\epsilon_0}(\frac{1}{R_c^2} - \frac{r}{r_c^3}) \tag{2}$$

which coincides with the outer field given by equation (1) at the point $r = r_c = 2$ Mpc. The radial profile of $E(r)$ is shown in Figure 3 in the interval $0 \leq r \leq 10$ Mpc. For example, at the distance $r = r_c$ = 2 Mpc the field strength is, $E(2Mpc) = 6.09$ V/m.

Electric field strengths computed by this model and standard values given above, range from -16.5 $milliVolt/m$ at the radial distance $r = 0$ (cluster center) up to 6.09 V/m at the cluster radius $r = r_c$ = 2 Mpc. Beyond this distance the field decreases according to equation (1). The dip around r = 2.2 kpc, where the field strength vanishes, is a visual effect of the logarithmic scale in the field intensity. The direction of the electric field in the radial region $r \leq 2.22$ kpc points at outward while for $r \geq 2.22$

[2] Consider two equal masses m retaining the same electric charge q (see fig. 1 in [4]. They experience an electrostatic repulsion and, at the same time, a gravity pull. Equilibrium or balance between the two forces occurs when the charge-to-mass ratio is $q/m = (4\pi\epsilon_0 G)^{1/2} = 8.617465 \times 10^{-11}$ C/kg where $\epsilon_0 = 8.8541 \times 10^{-12}$ F/m and G = 6.67 42 86 $\times 10^{-11}$ m^3/s^2 kg. The definition of balance charge q_b (b for balance) is, $q_b \equiv m\ (4\pi\epsilon_0 G)^{1/2}$ and, in turn, $\zeta_c \equiv q/q_b$. The dimensionless charge, ζ_c, is devoid of any subtlety. For example, the balance charge of the *Galaxy* is $M\ (4\pi\epsilon_0 G)^{1/2} = 2.5852 \times 10^{31}$ C where $M = 3.0 \times 10^{44}$ g = 15×10^{10} M_s is an arbitrary *Galactic* mass. Yet, the balance charge of the *Sun* is, $M_s\ (4\pi\epsilon_0 G)^{1/2}$ = 1.7139×10^{20} C where $M_s = 1.9884 \times 10^{33}$ g.

 doi:10.20944/preprints202602.1430.v1

kpc inward. The central volume designated as cluster *Niche* lies inside the yellow curve featured by $r \leq 2.22\ kpc$.

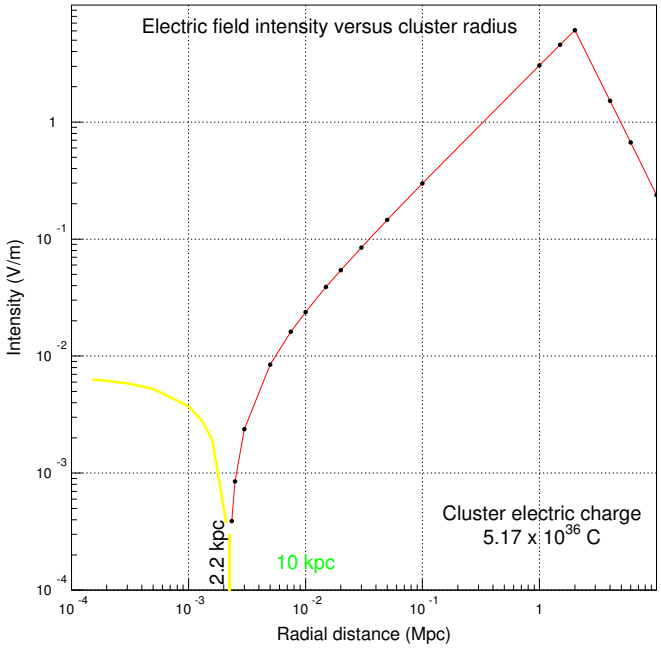

Figure 3. Electric field intensity versus radial distance of a generic galaxy cluster computed with the model termed double sphere with zero charge introduced elsewhere [25,26]. The parameters of the cluster are : $M_c = 2 \times 10^{47}\ g$, $r_c = 2\ Mpc$, $R_c = 150\ Mpc$, $\zeta_c = 150$ and $Q_c = \zeta_c\ M_c\ 0.8617 \times 10^{-11} = 5.17 \times 10^{36}\ C$. Electric field strength ranges from -16.5 $milliVolt/m$ at the radial distance r = 0 (cluster center) up to 6.09 V/m at the cluster radius $r = 2\ Mpc$. Beyond the distance r_c the field decreases according to equation (1). The dip around $r = r_c = 2.22\ kpc$, where the field strength vanishes, is a visual effect of the logarithmic scale. The direction of the electric field in the radial region $r \leq 2.22\ kpc$ points at outward while for $r \geq 2.22\ kpc$ inward. The central volume designated as cluster *Niche* lies inside the yellow curve.

The radial profile of the electrostatic potential related to the electric field represented by equation (1) and (2) , in the same conditions specified above, setting $D \equiv Q_{rc}/4\ \pi\ \epsilon_0\ r_g = 7.529 \times 10^{23}\ V$ takes the form:

$$V_e(r) = D(-\frac{r_g}{r} - \frac{r}{n^2 r_g} + \frac{2}{n}) \quad (3-a) \qquad V_e(r) = D(-\frac{3}{2} + \frac{2}{n} - \frac{r}{n^2 r_g} + \frac{r^2}{2r_g^2}) \quad (3-b)$$

where $n \equiv R_c/r_c$. Equation (3-a) holds for $r_c < r < R_c$ while the (3-b) for $0 < r < r_c$. The classical normalization condition of zero electrostatic potential at very large distances has been adopted.

4. A Linear Array of Galaxy Clusters in a Bath of Cosmic Rays

A linear array of N galaxy clusters is shown in Figure 4-a. It is a highly schematic distribution of galaxy clusters for the present calculation. Consider a chain of N galaxy clusters placed on a straight line at the typical average, constant distance, d_c (c for cluster). Let us set N=30 and $d_c = 60\ Mpc$. At the extreme end of the chain lie peripheral clusters which populate low density regions (referred to as voids) designated by region V_A and region V_B (Figure 4-a). It is intuitive that these peripheral clusters precipitate at high velocity toward the two extreme ends of the chain due to the voids V_A and V_B. For this reason these clusters are also termed *precipitating clusters*. The extreme peripheral cluster A_{-33} has initial coordinates x = -1950 Mpc while the cluster A_{33} has initial coordinate : x = +1950 Mpc. The origin of the reference frame is at half distance between clusters A_{-1} and A_1 (Figure 4-b). The length of

 doi:10.20944/preprints202602.1430.v1

the cluster chain L from A_{-33} to A_{33} is, $L = 2\,N d_c = 3900\ Mpc$, about 12.7 billion light years. The void V_A designates the zone around the extreme galaxy cluster A_{-33} while the void V_B that around the cluster A_{33}.

A giant cloud of cosmic rays carrying positive electric charge develops around the cluster filament following the arguments reported elsewhere (*Segment* 7.1 ref. [5]). This charged halo is qualitatively represented by red dots in Figure 4-b. During the *Hibernation Era* the dynamic status of the clusters is dominated by gravity and cosmic microwave radiation .

Let be $R(t)$ the total length of the filiform chain at the generic time t. At $t = 0$ it is : $R(0) = L = 2\ N\ d_c = 3900\ Mpc$ and, of course, as time progresses, $R(t_2) \geq R(t_1)$ being $t_2 \geq t_1$ due to the electrostatic repulsion.

As long as negative electric charge is released by single galaxies and confined within the cluster volume of radius r_c and, concomitantly, cosmic nuclei overflow beyond the radius r_c, any pairs of contiguous galaxy clusters will experience the electrostatic repulsion, as debated in ref. [4] for two clusters. The electrostatic repulsion is visualized in Figure 1 and 2. Red dots in these two figures represent the expanding positive charged halo of cosmic nuclei. The variable distance between any two adjacent clusters at the generic time interval t is designated by $d_c(t)$. Because the two voids V_A and V_B occupy symmetric positions (Figure 4-a) and cosmic nuclei overflow into these voids, as time progresses, the amount of unbalanced negative electric charge retained within cluster radii will augment.

Concomitantly, the total length $R(t)$ of the cluster chain increases from its

initial length of 3900 Mpc. Thus, the distance r will grow going from central to peripheral clusters.

In the following is adopted a suitable unit of acceleration denoted by a_u. The unitary acceleration is that experienced by two galaxies of equal mass $m_g = 3 \times 10^{44}\ g$ placed at the arbitrary distance d of 1 Mpc caused only by gravity. Accordingly it is, $a_u \equiv G\ m_g / d^2 = 2.102 \times 10^{-14}\ msec^{-2}$ where G is the gravitational constant and $m_g = 3 \times 10^{41}\ kg$. Adopting this acceleration unit the acceleration of a generic cluster caused both by gravity [3] and electrostatic forces on nearby adjacent clusters simplifies. Notice that accelerations experienced by clusters are in the range 10^{-10}-$10^{-14}\ m/s^2$, quite insignificant to the terrestrial $g = 9.8\ m/s^2$.

Let assign a series of N galaxy clusters with accelerations $a_1, a_2, ..., a_N$. The acceleration a_1 of the first cluster A_1 is given by :

$$a_1 = a_u \frac{g_2(\zeta_1\zeta_2 - 1)}{d_{1,2}^2} + \frac{g_3(\zeta_1\zeta_3 - 1)}{d_{1,3}^2} + \frac{g_4(\zeta_1\zeta_4 - 1)}{d_{1,4}^2} + ... \tag{4}$$

where ζ_n is the electric charge of the $n-th$ cluster, g_n the number of galaxies in the $n-th$ cluster and $d_{n,k}$ the distance between the $n-th$ and $k-th$ clusters.

Cluster charges Q_{gc} are expressed in units of balancing charge Q_b^c being $\zeta_c \equiv Q_c / Q_b^c$. Similarly to calculation parameters adopted in ref. [4], it is : $M_n = N_g m_g = 2500 \times\ 3 \times 10^{44} = 7.5 \times 10^{47}\ g$, namely, a rich cluster has 2500 galaxies. All the masses of the cluster chain are equal, i.e. $N_g = 2500 = g_1 = g_2 = g_3 ... = g_N$ and also balancing charges, $\zeta_c = 150 = \zeta_1 = \zeta_1 ... \zeta_N$ are set equal. In equation (4), for conciseness, ζ_c has been abbreviated ζ_1, ζ_2 etc without c on foot. In the non relativistic approximation the mass m_n is constant.

---

[3] In *Relativistic Mechanics* the force, f_{rm}, acting between two galaxies of mass m and M, with $M \gg m$ might be expressed by: $f_{rm} = G\ M\ m\ /\ d_l^2\ (1 - A^2)$ where d_l is the distance between M and m measured by local rods, $A = 2GM/dc^2$, c is the light velocity and d is the distance between m and M feigning M extremely small. With $M = 3 \times 10^{41}\ Kg$ and $d = 0.5\ Mpc$ (typical values) it results, $A \sim 10^{-7}$ which is a negligible correction to the force $f = G\ M\ m\ /\ r^2$ in *Classical Mechanics*.

 doi:10.20944/preprints202602.1430.v1

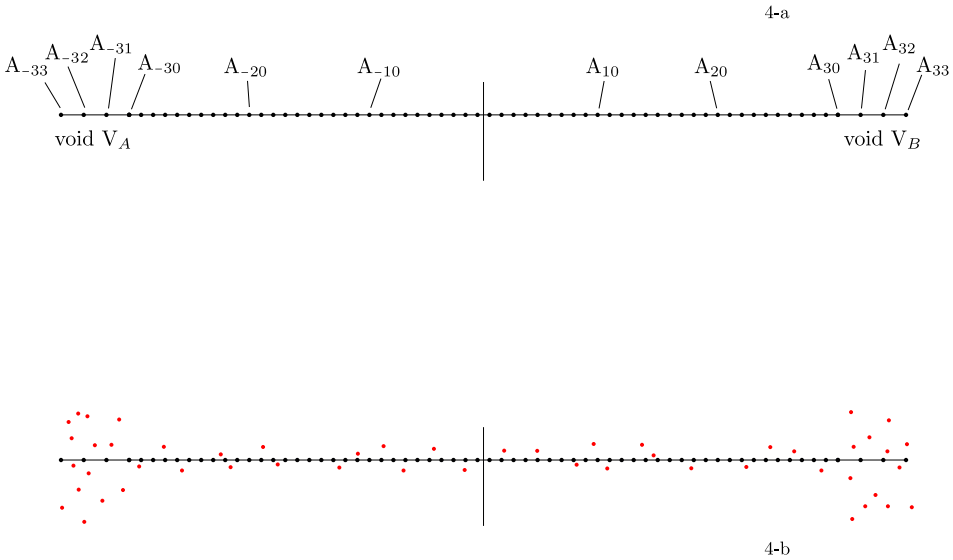

Figure 4. Ideal threadlike chain of galaxy clusters placed at the initial constant distance d_c of 60 Mpc aligned onto the x axis at the origin Ω placed inbetween a the clusters A_{-1} and A_1. At the two extreme ends of the chain there is a jump in the matter density. This filiform chain consists of 66 galaxy clusters, from A_{-33} to A_{33}, extending across 3900 Mpc (12.7 *billion of light years*). (4-b) Halo of cosmic nuclei (red dots) surrounding the filiform chain of galaxy clusters.

Repulsive forces among clusters shrink or compress mutual initial distances in an absolutely different way, depending if the cluster is in a central position or a peripheral position. In this respect consider the generic cluster A_n in the central zone of the filament shown in Figure 4-a. Let f_l (l for left) denote the intensity of the total electrostatic force exerted by the cluster A_n directed toward the left and f_r (r for right) the force directed toward the right.

As long as the positively charged halo of the cosmic nuclei propagates (to comprehend in a flash consider red dots in Figure 1 and 2 and 4-b) the cluster A_n suffers the effect of the repulsive force f_l exerted by the clusters A_{n+1} A_{n+2}, A_{n+3}, ..A_{33} situated in the region to its right. Likewise, a repulsive force f_r is generated by the clusters A_{n-1} A_{n-2}, A_{n-3}, ... A_{-33}, placed on the left region of A_n (Figure 4-b). Clusters lying in the central zone of the filiform chain develop comparable forces f_l and f_r e.g. : $f_l \simeq f_r$ due to the cluster chain symmetry.

The time behavior of the acceleration of a number of clusters (A_2, A_3, A_7, A_{11}), caused by the repulsive forces for a time span of 30 Ga are shown in Figure 5. One easily realizes that the acceleration initially increases, then reaches a maximum and then yet decreases smoothly. This characteristic profile derives from two opposite effects : the dissemination of positive electric charge in larger and larger regions promotes an increasing repulsive electrostatic force of negative charges in clusters. But at the same time, mutual distances among clusters increase, causing a decrement of the repulsive force. At short time intervals prevails the repulsion while at long time intervals dominates the attenuation due to larger and larger distances between clusters.

These basic characteristic features are expressed by equation (4) and displayed in Figure 5 (cluster acceleration versus time).

A thoroughly different condition looms out at the extreme end of the cluster chain where forces exerted on the peripheral clusters are definitely unbalanced i. e. well out of equilibrium. Indeed, the force f_l existing on the peripheral clusters closed to the void V_A is enormous, because of matter depression, while f_r is very modest. The large disparity of the forces $f_l \neq f_r$ produces large accelerations on peripheral clusters which gain velocities, always directed toward the exterior i.e. toward the low density region. That translates in increasing displacements with increasing time which, in turn, entails the dilatation of the cluster chain $R(t)$ at the time t with respect to the initial cluster length, $L \equiv R(0)$ =3900 Mpc for t = 0.

 doi:10.20944/preprints202602.1430.v1

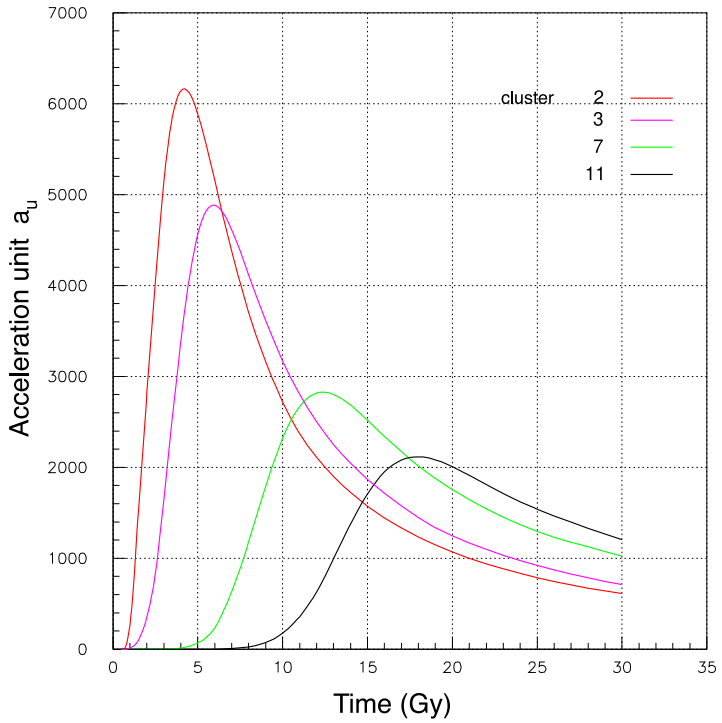

Figure 5. Acceleration of galaxy clusters as a function of time for the filiform chain of clusters represented in Figure 4 in units $a_u = 2.102 \times 10^{-14}\ m/s^{-2}$. Forces are very intense but well balanced in the central clusters so that accelerations are modest (black curve). Forces are also very high in the peripheral clusters but out of balance and, consequently, yield very large accelerations (red and magenta curves). The acceleration of the cluster A_1 (not shown in this figure as it is out of scale) has a maximum of 9765 $a_u = 2.052 \times 10^{-10}\ m/s^{-2}$ reached at the time t = 2.7 Ga.

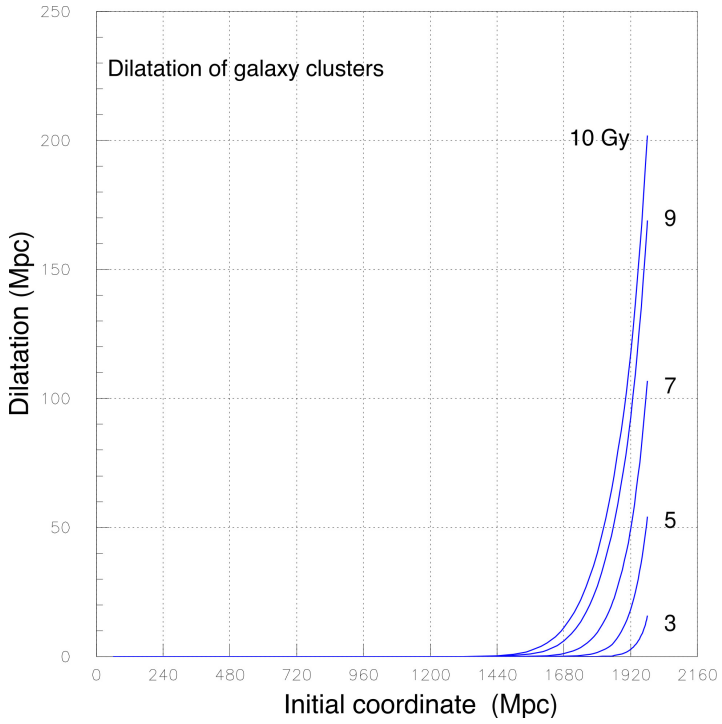

Figure 6. Velocity of galaxy clusters as a function of time until 30 Gy for the 7 peripheral clusters (A_1, A_3, A_5 A_7, A_9, A_{11}) of the treadlike chain. This acceleration profiles derive from the acceleration profiles shown in Figure 5.

 doi:10.20944/preprints202602.1430.v1

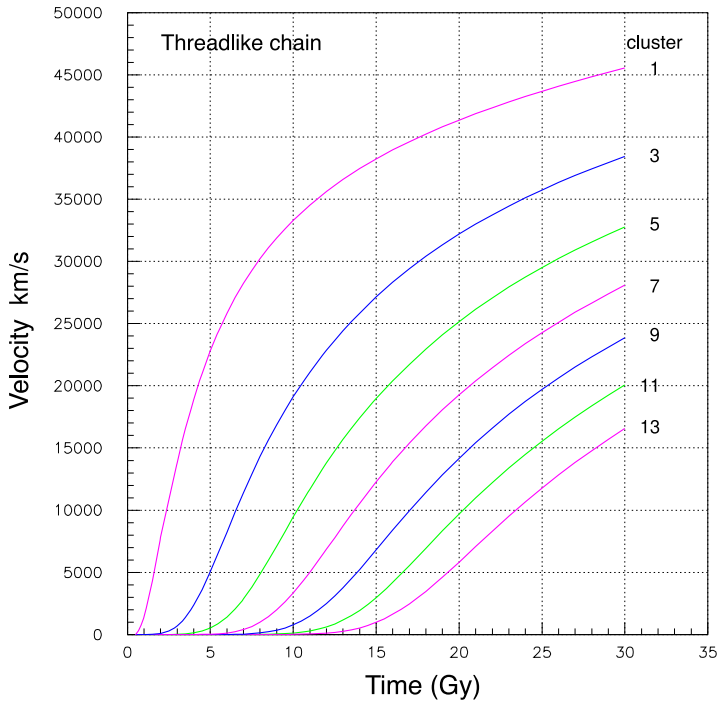

Figure 7. Straight line tracks traveled by the clusters of the threadlike chain versus initial positions after the time interval 3, 5, 7, 9 and 10 billion years (Gy). The coordinate along the x axis are the initial positions relative to the origin Ω of the three galaxy clusters A_1, A_2, A_3, ... up to the extreme cluster A_{33} which has initial coordinates of 1950 Mpc (see Figure 4-a). The other half of the galaxy clusters having symmetric positions from A_{-1} to A_{-33}, with initial negative coordinates from x = -30 Mpc for A_{-1}) etc and x = -1950 Mpc for A_{-33} is not shown as it has exactly the symmetric profiles.

The velocity v_x gained by the cluster at the time t due to the acceleration a_x is given by :

$$v_x = \frac{a_x t + \gamma_I \beta_I^x}{\sqrt{1 + (a_x t + \gamma_I \beta_I^x)^2 / c^2}} \tag{5}$$

where a_x is the acceleration along the x axis, γ_I and β_I the relativistic parameters of the initial status of the cluster at the input of the acceleration region, $\beta_I = v_I/c$ and γ = (1. -β^2)$^{-1/2}$. Velocity versus time until to 30 Gy are shown in Figure 6. Obviously, trajectory lengths traveled by clusters may be calculated once cluster velocities are known and as well the global dilatation of the cluster filament $R(t)$ at the time t.

Dilatations are expressed by the variations of the cluster coordinates. At the generic time interval t the difference in the coordinates of two contiguous clusters, x_{-k+1} - x_{-k} with k delimited in the range $-32 < k < 33$ defines the dilatation between any pair of clusters.

Hence it is : d_k (t) = x_{-k+1} - x_{-k} where the time dependence in x_{-k} and in x_{-k+1} is omitted for conciseness. The dilatations d_k (t) are shown in Figure 7 for two time intervals t_1 = 1 billion years and t_2 = 5 billion years. Notice that central clusters have very small dilatations but velocities are conspicuous. Peripheral clusters have enormous velocities in the range 30 000-45 000 km/s.

The dynamic status of this simple, ideal system has other notable properties. The profiles of the velocities of all the clusters of the chain of three different reference frames are shown in Figure 8 for three initial cluster positions along the chain : central, intermediate and extreme. They are the relative velocities of all clusters in the reference frames

placed to the clusters A_{33} (extreme), A_{20} (intermediate) and A_9 (central).

 doi:10.20944/preprints202602.1430.v1

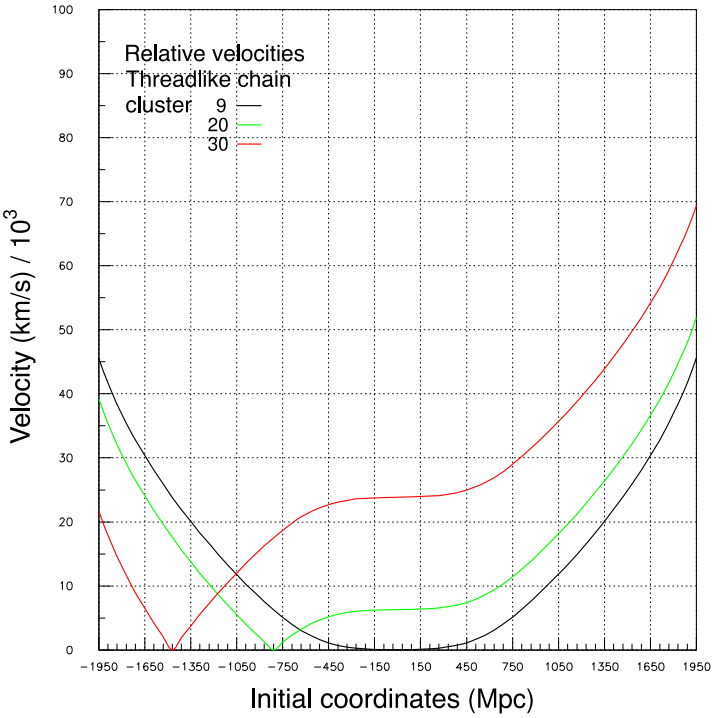

Figure 8. Cluster velocities expressed in three different reference frames positioned in particular clusters of the filiform chain : (a) the central cluster A_9 (black curve); (b) the intermediate cluster A_{20} (green curve) ; (c) the peripheral cluster A_{30} (red curve). The three galaxy clusters, A_9, A_{20} and A_{30} (see Figure 4-a) are placed at the initial coordinates, -530, -780 and -1500 Mpc, respectively. Final coordinates are : -545, -848 and -1795 Mpc and velocities 45000, 51000 and 68000 Km/s, respectively.

The behavior of the velocities of the central cluster (black curve) is symmetric, while the velocities of the intermediate cluster (green curve) and peripheral cluster (red curve) are asymmetric. The curves in Figure 8 have concave profiles with maximum velocities taken up by the peripheral clusters. Minimum velocities instead are found at the bottom of the concave profile. The origin of the reference frame which by definition has zero velocity is set at the bottom of the concave profile. In the previous specified conditions the concave profile is a simple predictable kinematical effect.

The ensemble of the velocities constitute a smooth, regular distribution, which from the minimum (zero velocity) attains the maximum velocity v_{max}. Peripheral clusters attain the highest velocities while central clusters, instead,

very modest velocities, almost zero velocities. These results are quite plausible and intuitive once the existence of electrostatic fields $\vec{E}_c$ with intensities in the range estimated in ref. [3] is posited.

In summary, the essential properties of this ideal filiform chain of galaxy clusters (1), (2), (3), (4) are : (1) spatial dilatations d_k (t) rather modest (Figure 7) even for outlying clusters (called here also precipitating clusters) relative to the total length of the chain of 3900 Mpc. For example, the extreme cluster A_{33} during 10 Ga experiences a dilatation of about 200 Mpc passing from the coordinate $x_{33}(0)$ = 1950 Mpc to $x_{33}(10\ Ga)$ = 2150 Mpc being $d_3(10\ Ga) \equiv x_{33}(10\ Ga)$ - $x_{33}(0)$. (2) Almost unchanged distances of the clusters occupying the central zone of the chain as a function of time. Almost unchanged distances relative to the initial positions (see Figure 7). For example, the initial distance of 60 Mpc between two central clusters becomes 68 Mpc after 15 Ga of electrostatic repulsion. (3) Galaxy clusters situated at the extreme ends of the chain rapidly reach maximum velocities as previously noted ; (4) concave profiles of the relative velocities as shown in Figure 8.

 doi:10.20944/preprints202602.1430.v1

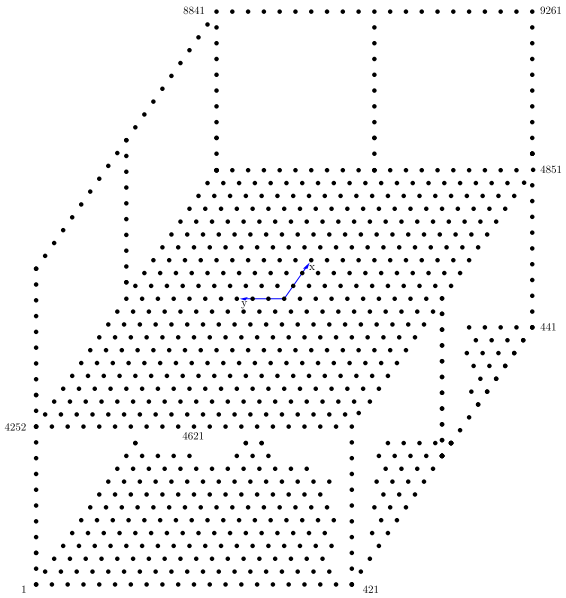

9-a

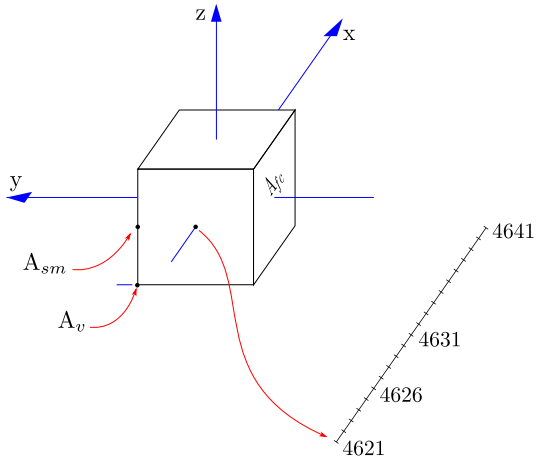

9-b

Figure 9. Material structure of 9261 galaxy clusters marshaled in a cube of side 1260 Mpc (about 4 *billion light years*). Both the cubic structure and the number of clusters is arbitrary. 9-a A cubic side hosts 21 clusters so that the total number of clusters is $21^3 = 9261$. Initially, distance d_c between adjacent clusters is the same, i. e. $d_c = 60\ Mpc$. 9-b A suitable scheme to identify clusters in the cubic array is shown. Extreme clusters A_{cf}, A_{sm} and A_v along with those along any straight-line segment (11 clusters) are indicated. Segments go from the center (cluster 4631) to the extreme end (cluster 4621).

5. Kinematic Properties of a Globe of Galaxy Clusters

The results of the filiform chain in the previous *Section* 3 are extended here to a three dimensional globe of galaxy clusters. Notable kinematical properties of 9261 galaxy clusters arranged in a cube of side 1260 Mpc (Figure 9) are calculated. The choice of this geometrical form is arbitrary but convenient for the numerical calculation. This geometrical form may be extrapolated to even larger matter aggregates in the range 1-10 Gpc. It may be anticipated here that the results of these calculations confirm the essential albeit highly schematic calculations reported in ref. [3] and in *Section* 4 of this work : Plus ça change et plus reste la même chose.

Consider an ordered array of galaxy clusters arranged in a cube as portrayed in Figure 9. Along a cube side there are N_c galaxy clusters. Each cluster equidistant from the nearby clusters at equal distances d_c of 60 Mpc. A cube side measures, $N_c\ d_c = 1260\ Mpc$ having arbitrarily fixed $N_c = 21$. Thus, there are 9261 galaxy clusters in the cube. The cube can be regarded as an ideal example of *clod*

 doi:10.20944/preprints202602.1430.v1

of matter[4] of very small size with average matter density $(N_g \times m_g) / (N_c d_c)^3 = 1.1 \times 10^{-31}\ g/cm^3$ where $N_g = 2500$ and $m_g = 3 \times 10^3\ g$ as previously stated.

In the calculations to follow the propagation of cosmic nuclei overflowed from galaxy clusters is described by the same profile adopted elsewhere (in *Section* 7.2, profile *c* in fig. 19 of ref. [4]).

The intensity of the electrostatic force on the generic cluster $k-th$ of the cube is governed by the adjacent number of clusters. The number of clusters contributing to the repulsive force at an arbitrary point within the cube exceeds that causing the repulsive force of the filiform chain of clusters of Figure 4 regardless of the matter density in the two structures. As a rule, due to this property, accelerations of the peripheral clusters in the cubic globe are greater than those of the peripheral clusters of the filiform chain. Thus, it is natural that accelerations and dilatations in the cubic array are expected to be larger than those of the filiform chain.

Maximum repulsive forces are experienced by the peripheral clusters designated by A_{cf} (cf for central face), A_{ms} (ms for medium side) and A_v (v for vertex). The coordinates of these clusters are shown in Figure 10. Void regions surround peripheral clusters characterized by notable gaps in matter density. Accelerations as a function of the time are smooth functions, similar to those shown in Figure 5 regarding the filiform chain. For instance, the acceleration peak of the cluster A_{cf} has an intensity of 29 170 a_u attained at the time of 2.18 Gy. Let us remind that a_u is the acceleration unit equal to $2.102 \times 10^{-14}\ ms^{-2}$ introduced in *Section* 4.

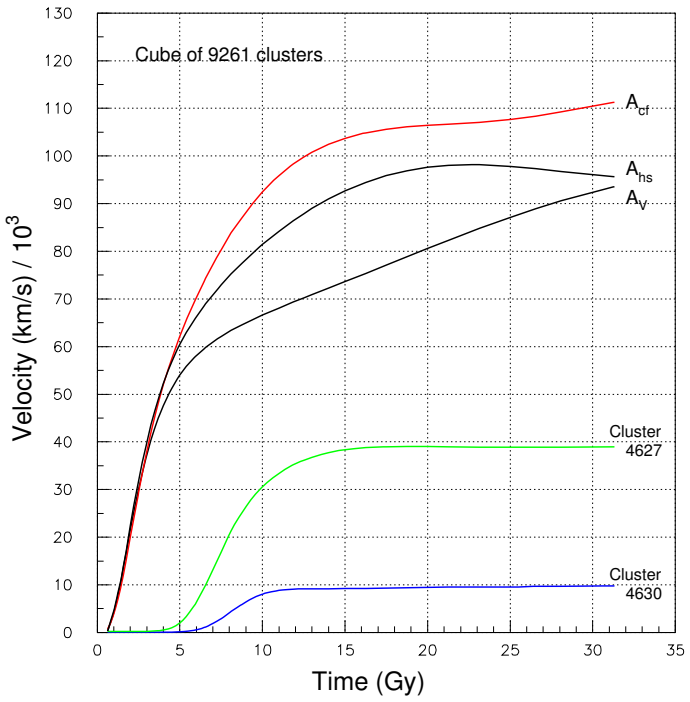

Figure 10. Velocity of some galaxy clusters arranged in a cubic array as a function of the time up to 30 Gy. Peripheral clusters A_{fc}, A_{sm} and A_v acquire velocities (black curves) greater than intermediate clusters (green curve, cluster 4627) and central clusters (blue curve, cluster 4630).

Velocity as a function of the time of the three peripheral clusters A_{fc}, A_{sm} and A_v are shown in Figure 10 in the time range, $0 \leq t \leq 30$ Gy. The terminal velocity of the cluster A_{cf}, that at 30 Gy,

[4] One might speculate that the nearby universe of mass $\sim 4 \times 10^{53}\ kg$ cannot be the sole matter aggregate around the Earth. Many other matter aggregates could exist at larger distances, for example in the range 10^{27}-$10^{28}\ m$. Any of these matter aggregates are called *clod* in ref. [5]. A clod with a mass $\sim 4 \times 10^{53}\ kg$ at the arbitrary distance of $10^{27}\ m$ would precipitate by gravity toward the local universe or *local clod* with an acceleration of $\sim 2 \times 10^{-14}\ m/s^2$

 doi:10.20944/preprints202602.1430.v1

is 111 370 Km/s. This velocity is greater than that of any other clusters of the clod and is explained by the elevated accelerations relative to the cluster A_{sm} and A_v and also relative to the rest of the clusters. Unsurprisingly, velocities and accelerations of the central clusters turns out to be inferior to those of the peripheral clusters. The velocity profile of an intermediate cluster is shown in Figure 10 (cluster 4627, green curve). Acceleration, velocity and dilatation of the very central cluster of the cube are null due to the symmetry of the cube array. Instead, the six clusters immediately closer to the central cluster of the cube, placed at the initial distance of 60 Mpc, have terminal velocities of 9772 Km/s, dilatations of 223 Mpc and acceleration maxima of 3718 a_u reached at 8.1 Gyr. The velocity profiles of these clusters are also shown in Figure 10 (blue curve, cluster 4630).

Similarly to the dilatation of the filiform chain, also a three dimensional dilatation of the generic *k-th* cluster of the clod may be defined using the difference between the initial position x_I, y_I and z_I and the final position attained at the generic time instant t, quantified by the coordinates x_k, y_k and z_k, that is :

$$d_k(t) = \sqrt{((x_k - x_I)^2 + (y_k - y_I)^2 + (z_k - z_I)^2)} \tag{6}$$

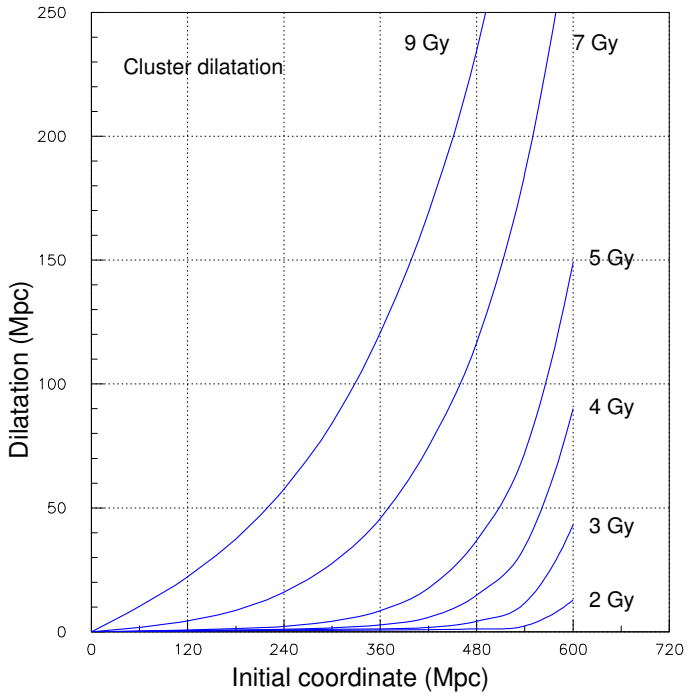

Figure 11. Distances travelled by 11 clusters in the cubic structure of Figure 9 from their initial positions as a function of the time at t = 2, 3, 4, 5, 7 and 9 *billion years*. The 11 galaxy clusters lying along a side of the cube are identified by their initial coordinates, which ranges from 60 Mpc to 600 Mpc (see Figure 9-b) and are initially positioned in a rectilinear segment. The final coordinates allow to visualize the dilatation of the cubic structure as a function of the time.

The trend of dilatations of cluster distances of the cube calculated according to equation (6) are reported in Figure 11. Maximum dilatations take place in peripheral clusters and, as soon as the central zone is involved, the dilatations become very modest. Zero dilatation occurs for the cluster at the center of the cube at the time t = 2 Ga. Temporal profiles of the cluster dilatations of the cube (Figure 11) imitate those of the filiform chain (Figure 7) but, as expected, have a larger magnitude.

The cluster velocities in diverse frames of reference are shown in Figure 12.

 doi:10.20944/preprints202602.1430.v1

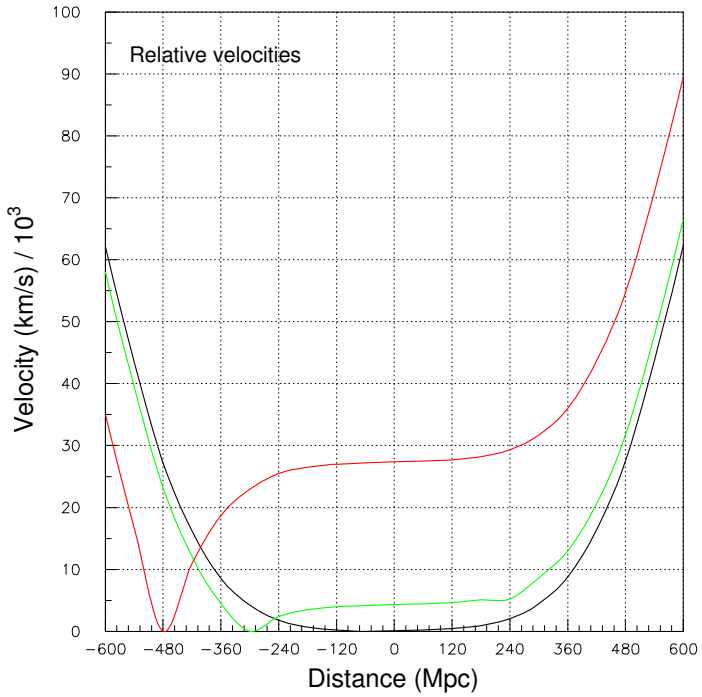

Figure 12. Cluster velocities expressed in three different reference frames glued to the particular clusters of the cube array : (a) the central cluster (black curve); (b) and intermediate cluster (green curve) ; (c) peripheral cluster (red curve). The three clusters are, respectively, A_{4630}, A_{4626} and A_{4623} (see Figure 9-b) positioned at the initial coordinate x of -60, -240 and -420 Mpc.

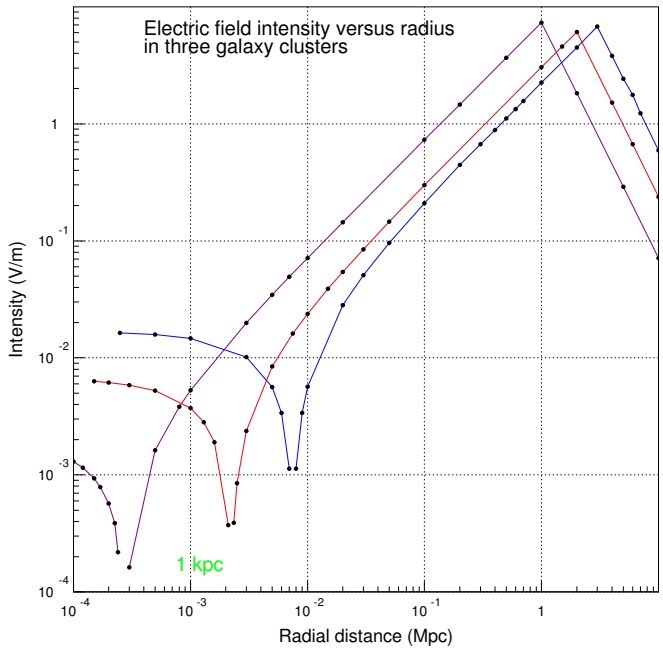

Figure 13. Radial profiles of the electric fields of three generic, rich, virialized galaxy clusters of mass 6.0×10^{47} g (blue curve), 2.0×10^{47} g (red) and 6.0×10^{46} g (violet) arbitrarily chosen. The spherical *Niche* boundaries of these three highly schematic clusters are located, respectively, at the radii of 7.5 kpc, 2.2 kpc and 0.277 kpc displayed in the figure as dips in the electric field profiles due to the logarithmic scale.

 doi:10.20944/preprints202602.1430.v1

These frames are positioned on a central cluster (black curve), an intermediate cluster (blue curve) and a peripheral cluster (red curve). It is apparent that cluster velocities display concave profiles analogously to the filiform chain (Figure 8).

Field galaxies or isolated galaxies surrounding clusters have not been included in the calculation to reduce computing times. Plausibly, the total positive and negative electric charge within an adequate distance from the isolated galaxy center is close to zero and, consequently, nearby cluster electric fields $\vec{E}_c$ exert negligible effects.

6. Compendium and Conclusions

The investigation of cosmic rays in galaxy clusters leads to the conclusion that the negative charge Q_{gc}^{-}, some 10^{34}-10^{36} C, resides within the radii of rich galaxy clusters while the corresponding positive charge, Q_{gc} = - Q_{gc}^{-} is spread out across the intercluster space as vividly displayed in Figure 2. These disjoint distributions of positive and negative charge generate steady electrostatic fields designated by $\vec{E}_c$ (c for cluster). In a simplified but essential calculation in 2021 [4], it was shown that electrostatic fields of two rich clusters overwhelm gravity attraction yielding a repulsive acceleration. This paper progresses along this exploration and reports the electrostatic expansion and acceleration of the *universe* using two galaxy cluster models arranged on a straight line of arbitrary length of 3900 Mpc and a three dimensional array of cubic form with matter density of 1.1×10^{-31} g/cm^3 and a total mass of 0.69×10^{52} g. The same work [4] has established that field galaxies have negligible electrostatic fields relative to those of clusters implying the dominant role of galaxy clusters in the acceleration of the *universe*.

The indicative mass and size of the *universe* appropriate for this work has been delineated in *Section* 2 [15]. From the computed velocities of two rich clusters [4], those of the linear array of 3900 Mpc and those of the cubic globe of 9261 galaxy clusters, it is possible to extrapolate the acceleration and expansion of the *universe*. Space displacements, velocities and accelerations of galaxy clusters from their initial positions, D_I are explicitly reported in *Section*4 and 5. A notable result is that the distances of galaxy clusters from the origin (see Figure 4 and 9) depend both on the initial position D_I and velocity v, namely, $D(v) = D_I + k\,v$ where k a strong function of the velocity. The dominant cosmology posits $D_I = 0$ and k constant in the entire range, $0 \leq v \leq 299\,792\ km/s$. These two hypotheses radically differ from those of this work and they deserve the elucidation given in the *Appendix* B.

Notice that current cosmology, originated in 1927 with the *primeval atom* [14] along with all its variants developed during a century, does not offer a Physics explanation of the acceleration and expansion of the universe but only speculations, inconsistent with well established laws of Physics (see *Appendix* A).

Dark Energy is electrostatic energy generated by the dynamics of cosmic rays in galaxy clusters. Electrostatic energy derives from electric fields in galaxy clusters. The fields are generated by the separation of positive and negative electric charges. The separation implies that the relative positions of the charges is not a random occurrence or they are statistical fluctuations of charge but they are unambiguously determined by the motion of cosmic rays. In principle, the repulsive character might take place with positive charges in the cluster cores and negative charges in the cluster peripheries but x-ray, radio, optical, gamma rays and infrared data dictate the contrary, namely, negative cluster cores[5] of very and positively charged cosmic rays disseminated in the intercluster space. This assertion is amply debated and ascertained elsewhere (see *Section* 5.5, 6.1, 6.2; Appendix *A* and *B* of ref. [5]).

[5] According to equation (3) electrostatic fields in the cores of rich galaxy clusters point at toward the exterior while elsewhere they point at inward. The radius where the electric field inverts its direction is designated by L_{inv} and it is shown in Figure 3 and 13. This work and others [4,5] designate the spherical volume $(4/3)\pi\ L_{inv}^3$ as *Niche*. A notable feature of the radius L_{inv} is its independence from the electric charge Q_{gc}^{-}. For instance, the galaxy cluster with a radius 2 = Mpc, adopted for the results shown in Figure 3, has a *Niche* radius L_{inv} = 2.22 kpc. Electric fields are sources of energy. At cluster centers they account for the notorious cooling flow-problem as they refuel the X-ray emitting gas (see ref. [5], *Appendix A*.2). They also explain the universal dip of the radial temperature profile at cluster cores as argued elsewhere (see [5], *Appendix A*.2).

 doi:10.20944/preprints202602.1430.v1

The empirical basis of electric fields is multifaceted; it stems from the copious and variegated radio emission in galaxy clusters, the scarcity of Iron in the innermost zones of galaxy clusters over radii of 20-100 *kpc* from the centers, the explanation of the cooling-flow problem at cluster cores, the deficit of gravity force to retain galaxies known as *Dark Matter* problem, central temperatures colder than those observed in the cluster main body, the absence of gamma rays from galaxy clusters at the expected rates and other data.

Gamma rays are not observed because cosmic-ray protons evaded from the clusters at the early times of the *Electrostatic Era* (see *Section* 2). Consequently, the nuclear reaction cosmic-ray proton off Hydrogen in the cluster volume, going into neutral pions and gamma rays does not occur at the predicted rates of about 10^{-8}-10^{-9} $photons/cm^2\ s$ [27,28]. For example, upper limits at 95 per cent confidence level of the undetected gamma-ray flux for 75 galaxy clusters in the range 0.8-100 GeV is 3×10^{-11} photons$/cm^2\ s$ [7]. This measurement agrees with other upper limits [6,29–32] in wider energy intervals. This severe mismatch is known since 2003 [8] and it persists at the present days with a gap of three orders of magnitude between observations and predictions. In this work the absence of cosmic-ray protons from galaxy clusters is regarded as a direct proof of negatively charged cluster cores and the existence of the electrostatic fields $\vec{E}_c$.

Electrostatic energy is not a generic source of energy as it might be the rest mass of hypothetical particles or non existing particles (for example, *chamaleons*, *dilatons*, *tachyons*, *symmetrons*, *axions*, *gravitons*) but it has also an intrinsic, repulsive character. In other respects, *Dark Energy* is a void notion in terms of elementary particles because the hypothetical particles of *Dark Energy* have never been detected though zealously sought.

The necessity of *Dark Energy* in the dominant unreal cosmology is the signature of a colossal, incurable error where the attractive gravity force is postulated to exclusively govern the motion of the giant material bodies around the *Earth* omitting the electrostatic fields generated by cosmic rays. In this context *Dark Energy* is a myth attesting something missing and real though in a false reasoning.

Appendix A A *Universe* of Geometrical Lines with Nothing Inside

The electrostatic acceleration of the *nearby universe* proposed in this work anchors on two prerequisites, namely : (1) the universe is not concentrated in a point (primeval fireball) as stipulated in the dominant cosmology but in a stretch of dimension 10^{26}-10^{27} m. (2) Galaxy clusters emerge from the *cold universe* at 2.725 *degrees* and are disseminated in the entire volume of the universe. Thus, the very initial dynamic status of the matter is quiescent, at low temperature and it is referred to as *Hibernation Era*. The quiescent matter can be only Hydrogen because no stars existed and no other heavier nuclei might have been produced.

These two prerequisites are not compatible with the dominant cosmology. How the cosmic microwave radiation was generated in a *cold universe* during the *Hibernation Era* is described in the forthcoming paper [33]: *A simpler explanation of the cosmic microwave radiation with a black body spectrum*.

The concepts of the dominant unreal cosmology (hereafter *DUC*) are frontally incompatible with the experimental laws of Physics and basic facts redundantly assessed by experiments and observations. Five of these unreal concepts (*UC*) are: (*UC*1) Objects running faster than light ; (*UC*2) the expansion of the space; (*UC*3) all the atoms piled up in a spatial point called *primeval fireball* or *primordial atom* [14]. (*UC*4) The universe age of 13.7 *Ga* instead of the longer ages resulting from the age observations of closed globular clusters of 20-25 *Ga* [9–13]. Moreover, precise observations of the remote regions of the universe have established that galaxies and larger matter aggregates are too mature and too large when confronted with the short age of 13.7 *Ga*. (*UC*5) The *primordial fireball* believed to be at arbitrary high temperatures, billion *degrees*, not at 2.725 *degrees*.

The reality of the *primordial fireball* is invalidated by the first and second laws of thermodynamics as noted by many physicists. It is also incompatible with *Nuclear Physics* data (see footnote 3 in ref. [5]). Hence, it is unreal, the *primordial fireball* never existed.

 doi:10.20944/preprints202602.1430.v1

Other themes regarding false concepts are omitted here but they are debated and repudiated in scientific documents by other physicists.

This state of facts entails the rejection of any deductions based on the *primordial fireball*. But supporters of the *DUC* believes to decrypt and explain the nature of the cosmic microwave radiation via the *primordial fireball*.

From this belief derives an example of logical monstrosity of the dominant cosmology. Optical photons in the *primeval fireball* are shifted by a factor 1100, in order to become microwave photons, those of the cosmic microwave radiation. The expansion of the space (*UC*2) would produce the photon stretching.

Some physicists, still arguing within the context of *DUC*, noticed that the most remote regions of the *universe* have the same temperature of 2.725 *degrees* with black body spectra but these remote regions have never interacted via massive particles or photons. Therefore, the equality of the temperature is surprising, unexpected, indecipherable. This conflict is called *Horizon Problem* and it is regarded as a serious problem for the *DUC* aficionados.

The reasoning generating the *Horizon Problem* is based on the premise (*UC*3) which is unfounded, and the expansion of space (*UC*2), which has no experimental basis either. But even feigning that both concepts (*UC*3 and *UC*2) are real facts, the conclusion is patently fake as it generates the *Horizon Problem*. Thus, there is no *Horizon Problem* but only an untenable, tortuous, unfortunate cosmology. The tough term, logical monstrosity, used in the *Appendix* B, refers this type of reasoning.

Note further that the cultural frame of the dominant cosmology is fragile and, perhaps, intrinsically obsolete. It has its roots in the *XIX* century. In that epoch physicists established the non existence of the *Ether*, the non existence of the *Caloric*, that light velocity is immune from the launching or braking platforms. It was also the century of geometrical lines seen in moving reference frames, when mathematicians enjoyed to deform the geometry of the ancient Greeks.

From the cultural background of the *XIX* century the *DUC* has inherited the concept of continuous fluid. Not atoms and elementary particles populate the *universe* but a continuous fluid decomposable in fragments of any sizes, indifferently, smaller or larger than the sizes of the elementary particles, which lie in the precise range 10^{-15}-10^{-16} m. It seems that the concept of continuous fluid facilitates the acceptance of the space expansion which is a vital tool of the *DUC* in the vain attempt to explain the cosmic microwave radiation of 2.725 *degrees*.

Physics has immensely progressed relative to the cultural frame of the *XIX* century. The chief advance in the *XX* century is the discover of the subatomic world teemed with about 10 000 nuclei and about 300 elementary particles, mostly in the range 0.1-11 GeV/c^2 precisely described by *Quantum Mechanics*. Only four elementary particles are stable : proton, electron, antiproton and positron. These real massive particles are the substance or essence of any conceivable *universe*. This was thoroughly unknown in the *XIX* century and it is not incorporated in the dominant unreal cosmology where any structureless mass is believed to be adequate; for example, masses in the *DUC* can be crammed into any arbitrary small volume whereas heavy ion collisions in particle accelerators attest maximum finite densities around 2.8×10^{-14} g/cm^3.

Appendix B Objects Running Faster than Light and All the Existing Atoms Piled Up in a Point

Physicists trying to dissect facts from fiction in the dominant cosmology (hereafter *DUC* for Dominant Unreal Cosmology) have a disagreeable task because this doctrine is ubiquitous at universities, radio facilities, astronomical observatories, space research centers and public fora.

Once two unreal notions have to cohabit because a third untenable idea imposes the cohabitation, a logical monstrosity may develop (see *Appendix* A). In this work the dominant cosmology is regarded as a scientific monstrosity, not only unreal. The first unreal notion is that all the objects of the *nearby universe* were amassed in a point or a small spatial region designated by *primeval atom* [14] or *primeval fireball*. For sake of clarity, let us denote here by Ω the location of the *primeval fireball* in a generic

 doi:10.20944/preprints202602.1430.v1

reference frame of *Classical Mechanics*. From the hypothesis of a homogeneous universe (see ref. [34] for an empirical test of this hypothesis) and the *Relativistic Mechanics* incorporated in the *DUC*, this location, within 12 000 Mpc, has no identifiable coordinates, which is insufferable.

The second unreal notion pertains a grand cosmic order of angelic origin where the distance from the *Earth* of all celestial bodies, $D(v)$, is simply proportional to the observed velocity v measured by the redshift of the spectral lines, namely, $D(v) = k\ v$ where k is a numerical constant, not a strong function of the velocity as it is displayed in Figure 8 and 12. For example, using the *Coma* cluster at a distance of 98.5 Mpc and a recession velocity of 7200 km/s, it turns out $k = 13.5\ pc/s$ and therefore, $D(kpc) = 13.5\ v(km/s)$. Notice that this correlation implicitly and essentially preassumes the *primeval fireball* [14] where about 10^{80} Hydrogen atoms with a mass of $1.6 \times 10^{53}\ Kg$ are crammed into a small region or a spatial point.

The correlation $D(v) = k\ v$ of the *DUC* is highly misleading and has created many artificial problems in the scientific community as argued below[6] .

The third untenable idea is the arbitrarily high temperature of the *primeval fireball*. The *DUC* posits that the cosmic microwave radiation at temperature of 2.725 *degrees* originates from the the *primeval fireball* believed to be at an arbitrarily high temperature, for instance, billion *degrees*.

Following the *DUC*, during the *primordial fireball* all the material bodies resided in the location Ω, exactly 13.7 Ga ago, and received from scratch an immense dose of kinetic energy in a very selective manner. The different doses of kinetic energy are postulated in such a way that the more kinetic energy the objects absorb, the more distant they travel from the origin $\Omega = 0$ or, equivalently stated, the accelerations of any objects at the common origin Ω are uniquely different.

For simplicity subdivide all the giant material bodies in five arbitrary classes : galaxy clusters, field galaxies, quasars, supernovae, galaxies in voids[7]. In this highly arbitrary scheme supernovae form a class because they are standard candles to measure distance beyond 100-400 Mpc and, of course, they follow the dynamics of the host galaxies. According to the *DUC* these five categories of objects presently displace, not in a unique, characteristic disorder, but they follow the precise correlation evoked above, namely, $D(v) = k\ v$ which in the previous example is : $D(kpc) = 13.5\ v(km/s)$.

Assume that the distance of galaxy clusters, D_{gc}, field galaxies, D_{fg}, supernovae D_{su}, quasars, D_{qu} and galaxies in voids, D_{gv}, obey the simplest five correlations in restricted velocity bands : $D_{gc} = I_{gc} + k_{gc}\ v$, $D_{fg} = I_{fg} + k_{fg}\ v$; $D_{su} = I_{su} + k_{su}\ v$; $D_{qu} = I_{qu} + k_{qu}\ v$, $D_{gv} = I_{gv} + k_{gv}\ v$. Here the constants I_{gc}, I_{fg}, I_{su}, I_{qu} and I_{gv} are the initial coordinates of these celestial bodies.

At the beginning of the *Electrostatic Era* galaxy clusters have an initial positioning based on observations of the average interdistances of galaxy clusters and the matter density. The cubic massive body of galaxy clusters displayed in figure 9 is a surrogate of these observations. Notice that in a universe of mass $4.928 \times 10^{53}\ kg$ (corresponding to a local density of $3.0^{-31}\ g/cm^3$) and size $1.179 \times 10^{26}\ m$, the number of galaxy clusters in a side of the cube of figure 9 would be 637 for a total of $637^3 = 2.58 \times 10^8$.

The initial positioning of the galaxy clusters admitted in this work differs from that of the *DUC*, which is $I_{gc} = I_{fg} = I_{su} = I_{qu} = I_{gv} = 0$ coincident with the *primordial fireball* located at the unmeasurable origin, $\Omega = 0$.

---

[6] The hypothesis that the macroscopic space of astronomical size expands *ad libidum* is not accepted in this work because it has no empirical basis. Direct empirical tests of space expansion, not phantasies, have never been accomplished though conceived or planned (see for example [35]). Atoms or elementary particles may shrink or enlarge in space according to physical laws established in laboratory. For example, atomic radii may change by the *Stark effect*.

[7] Galaxy clusters with their electric fields are the real motors of the universe acceleration and expansion as presented in this work and elsewhere [4,5]. Isolated galaxies (field galaxies), probed from distances overwhelming their sizes (actually the sizes of the positively charge clouds of cosmic rays) are electrically neutral and, therefore, they are not affected by the cluster electric fields. Such galaxies are trailed by gravity from the closest massive cluster. For example, the local group (Andromeda, Milky Way, Maffei I, M33 etc) suffers a gravity pull toward the nearest massive cluster, Virgo, at about 250 km/s. Quasars are exceptional galaxies with an electric charge exceeding that of normal galaxies by a factor 10-50 [5]. For this only reason they travel at recession velocities higher than galaxy clusters or field galaxies. Galaxies in voids not only are electrically neutral like field galaxies but, by definition, any galaxy clusters lie remote from them and, thus, even gravity is puny. These three classes of cosmic objects are expected to have the functions, $k_{gc}(v)$,$k_{qu}(v)$, $k_{gv}(v)$ different.

 doi:10.20944/preprints202602.1430.v1

A second hypothesis of the *DUC* dictates that, $k_{gc} = k_g = k_{su} = k_{qu} = k_{gv} = k$ namely, all the five different categories of celestial bodies travel in such a way to obey the smooth correlation, $D(v) = k\,v$ where k is a unique constant and not five different functions of the highly schematic example given above.

The results shown in Figure 8 and 12 demonstrate that the parameter k_{gc} cannot be a unique constant k for galaxy clusters which are the real motors of the universe acceleration and expansion.

Conflicts of Interest: The author declare no conflicts of interest.

References

1. Slipher, V.M. Radial velocity observations of spiral nebulae. *The Observatory* **1917**, *40*, 304–306.
2. Riess, A.G.; Filippenko, A.V.; Challis, P.; Clocchiatti, A.; Diercks, A.; Garnavich, P.M.; Gilliland, R.L.; Hogan, C.J.; Jha, S.; Kirshner, R.P.; et al. Observational Evidence from Supernovae for an Accelerating Universe and a Cosmological Constant. *Astronomical Journal* **1998**, *116*, 1009–1038, [arXiv:astro-ph/astro-ph/9805201]. https://doi.org/10.1086/300499.
3. Perlmutter, S.; Aldering, G.; Goldhaber, G.; Knop, R.A.; Nugent, P.; Castro, P.G.; Deustua, S.; Fabbro, S.; Goobar, A.; Groom, D.E.; et al. Measurements of Ω and Λ from 42 High-Redshift Supernovae. *ApJ* **1999**, *517*, 565–586, [arXiv:astro-ph/astro-ph/9812133]. https://doi.org/10.1086/307221.
4. Codino, A. On the overflowing of cosmic rays from galaxies and the expansion of cosmic matter. In Proceedings of the 37th International Cosmic Ray Conference, 2022, p. 150, [arXiv:astro-ph.HE/2109.04393]. https://doi.org/10.22323/1.395.0150.
5. Codino, A. *How electrostatic fields generated by cosmic rays cause the expansion of the nearby universe*; Published by Esculapio Publishing Company, Bologna, Italy, 2022.
6. Ackermann, M.; Ajello, M.; Albert, A.; Allafort, A.; Atwood, W.B.; Baldini, L.; Ballet, J.; Barbiellini, G.; Bastieri, D.; Bechtol, K.; et al. Search for Cosmic-Ray-induced Gamma-Ray Emission in Galaxy Clusters. *ApJ* **2014**, *787*, 18, [arXiv:astro-ph.HE/1308.5654]. https://doi.org/10.1088/0004-637X/787/1/18.
7. Griffin, R.D.; Dai, X.; Kochanek, C.S. New Limits on Gamma-Ray Emission from Galaxy Clusters. *ApJl* **2014**, *795*, L21, [arXiv:astro-ph.HE/1405.7047]. https://doi.org/10.1088/2041-8205/795/1/L21.
8. Reimer, O.; Pohl, M.; Sreekumar, P.; Mattox, J.R. EGRET Upper Limits on the High-Energy Gamma-Ray Emission of Galaxy Clusters. *ApJ* **2003**, *588*, 155–164, [arXiv:astro-ph/astro-ph/0301362]. https://doi.org/10.1086/374046.
9. Sandage, A. The age of the globular cluster system. *ApJ* **1982**, *252*, 553–573. https://doi.org/10.1086/159582.
10. Böhm-Vitense, E.; Szkody, P. The interpretation of the two-color and color-magnitude diagrams of M15 and M92. *ApJ* **1973**, *184*, 211. https://doi.org/10.1086/152320.
11. Jerjen, H.; Binggeli, B.; Barazza, F.D. Distances, Metallicities, and Ages of Dwarf Elliptical Galaxies in the Virgo Cluster from Surface Brightness Fluctuations. *Astronomical Journal* **2004**, *127*, 771–788, [arXiv:astro-ph/astro-ph/0310779]. https://doi.org/10.1086/381065.
12. Janes, K.; Demarque, P. The ages and compositions of old clusters. *ApJ* **1983**, *264*, 206–214. https://doi.org/10.1086/160587.
13. Fukugita, M.; Hogan, C.J. Global cosmological parameters. *European Physical Journal C* **2000**, *15*, 136–142. https://doi.org/10.1007/BF02683413.
14. Lemaître, G. Un Univers homogène de masse constante et de rayon croissant rendant compte de la vitesse radiale des nébuleuses extra-galactiques. *Annales de la Société Scientifique de Bruxelles* **1927**, *47*, 49–59.
15. Carvalho, J.C. Derivation of the mass of the observable universe. *International Journal of Theoretical Physics* **1995**, *34*, 2507–2509. https://doi.org/10.1007/BF00670782.
16. Ackermann, M.; Ajello, M.; Allafort, A.; Baldini, L.; Ballet, J.; Bastieri, D.; Bechtol, K.; Bellazzini, R.; Berenji, B.; Bloom, E.D.; et al. GeV Observations of Star-forming Galaxies with the Fermi Large Area Telescope. *ApJ* **2012**, *755*, 164, [arXiv:astro-ph.HE/1206.1346]. https://doi.org/10.1088/0004-637X/755/2/164.
17. Kornecki, P.; Pellizza, L.J.; del Palacio, S.; Müller, A.L.; Albacete-Colombo, J.F.; Romero, G.E. γ-ray/infrared luminosity correlation of star-forming galaxies. *A&A* **2020**, *641*, A147, [arXiv:astro-ph.HE/2007.07430]. https://doi.org/10.1051/0004-6361/202038428.
18. Garn, T.; Green, D.A.; Riley, J.M.; Alexander, P. The relationship between star formation rate and radio synchrotron luminosity at $0 < z < 2$. *MNRAS* **2009**, *397*, 1101–1112, [arXiv:astro-ph.GA/0905.1218]. https://doi.org/10.1111/j.1365-2966.2009.15073.x.

19. Shmaonov, T. *Pribori i Tekhnika Experimenta* **1957**, p. 83.
20. Tacconi, L.J.; Genzel, R.; Neri, R.; Cox, P.; Cooper, M.C.; Shapiro, K.; Bolatto, A.; Bouché, N.; Bournaud, F.; Burkert, A.; et al. High molecular gas fractions in normal massive star-forming galaxies in the young Universe. *Nature* **2010**, *463*, 781–784, [arXiv:astro-ph.CO/1002.2149]. https://doi.org/10.1038/nature08773.
21. Wang, R.; Wagg, J.; Carilli, C.L.; Neri, R.; Walter, F.; Omont, A.; Riechers, D.A.; Bertoldi, F.; Menten, K.M.; Cox, P.; et al. Far-infrared and Molecular CO Emission from the Host Galaxies of Faint Quasars at z ∼6. *Astronomical Journal* **2011**, *142*, 101, [arXiv:astro-ph.CO/1107.5065]. https://doi.org/10.1088/0004-6256/142/4/101.
22. Webb, T.M.A.; Lowenthal, J.; Yun, M.; Noble, A.G.; Muzzin, A.; Wilson, G.; Yee, H.K.C.; Cybulski, R.; Aretxaga, I.; Hughes, D.H. Detection of a Substantial Molecular Gas Reservoir in a Brightest Cluster Galaxy at z = 1.7. *The Astrophysical Journal Letters* **2017**, *844*, L17. https://doi.org/10.3847/2041-8213/aa7749.
23. Bowman, J.D.; Rogers, A.E.E.; Monsalve, R.A.; Mozdzen, T.J.; Mahesh, N. An absorption profile centred at 78 megahertz in the sky-averaged spectrum. *Nature* **2018**, *555*, 67–70, [arXiv:astro-ph.CO/1810.05912]. https://doi.org/10.1038/nature25792.
24. Juarez, Y.; Maiolino, R.; Mujica, R.; Pedani, M.; Marinoni, S.; Nagao, T.; Marconi, A.; Oliva, E. The metallicity of the most distant quasars. *A&A* **2009**, *494*, L25–L28, [arXiv:astro-ph.CO/0901.0974]. https://doi.org/10.1051/0004-6361:200811415.
25. Codino, A. *The ubiquitous mechanism accelerating cosmic rays at all the energies*; Published by Esculapio Publishing Company, Bologna, Italy, 2020.
26. Codino, A. Models and Formulae of the Galactic Electrostatic Field. *Preprints* **2025**. https://doi.org/10.20944/preprints202510.2074.v1.
27. Dennison, B. Formation of radio halos in clusters of galaxies from cosmic-ray protons. *ApJl* **1980**, *239*, L93–L96. https://doi.org/10.1086/183300.
28. Dar, A.; Shaviv, N.J. Origin of the High Energy Extragalactic Diffuse Gamma Ray Background. *Phys. Rev. Lett.* **1995**, *75*, 3052–3055, [arXiv:astro-ph/astro-ph/9501079]. https://doi.org/10.1103/PhysRevLett.75.3052.
29. Aleksić, J.; Alvarez, E.A.; Antonelli, L.A.; Antoranz, P.; Asensio, M.; Backes, M.; Barres de Almeida, U.; Barrio, J.A.; Bastieri, D.; Becerra González, J.; et al. Constraining cosmic rays and magnetic fields in the Perseus galaxy cluster with TeV observations by the MAGIC telescopes. *A&A* **2012**, *541*, A99, [arXiv:astro-ph.HE/1111.5544]. https://doi.org/10.1051/0004-6361/201118502.
30. Arlen, T.; Aune, T.; Beilicke, M.; Benbow, W.; Bouvier, A.; Buckley, J.H.; Bugaev, V.; Byrum, K.; Cannon, A.; Cesarini, A.; et al. Constraints on Cosmic Rays, Magnetic Fields, and Dark Matter from Gamma-Ray Observations of the Coma Cluster of Galaxies with VERITAS and Fermi. *ApJ* **2012**, *757*, 123, [arXiv:astro-ph.HE/1208.0676]. https://doi.org/10.1088/0004-637X/757/2/123.
31. Zandanel, F.; Ando, S. Constraints on diffuse gamma-ray emission from structure formation processes in the Coma cluster. *MNRAS* **2014**, *440*, 663–671, [arXiv:astro-ph.HE/1312.1493]. https://doi.org/10.1093/mnras/stu324.
32. Ackermann, M.; Ajello, M.; Albert, A.; Atwood, W.B.; Baldini, L.; Ballet, J.; Barbiellini, G.; Bastieri, D.; Bechtol, K.; Bellazzini, R.; et al. Search for Gamma-Ray Emission from the Coma Cluster with Six Years of Fermi-LAT Data. *ApJ* **2016**, *819*, 149, [arXiv:astro-ph.HE/1507.08995]. https://doi.org/10.3847/0004-637X/819/2/149.
33. Codino, A. A simpler explanation of the cosmic microwave radiation with a black body spectrum. to be submitted to Nature.
34. Migkas, K.; Pacaud, F.; Schellenberger, G.; Erler, J.; Nguyen-Dang, N.T.; Reiprich, T.H.; Ramos-Ceja, M.E.; Lovisari, L. Cosmological implications of the anisotropy of ten galaxy cluster scaling relations. *A&A* **2021**, *649*, A151, [arXiv:astro-ph.CO/2103.13904]. https://doi.org/10.1051/0004-6361/202140296.
35. Liske, J.; Grazian, A.; Vanzella, E.; Dessauges, M.; Viel, M.; Pasquini, L.; Haehnelt, M.; Cristiani, S.; Pepe, F.; Avila, G.; et al. Cosmic dynamics in the era of Extremely Large Telescopes. *MNRAS* **2008**, *386*, 1192–1218, [arXiv:astro-ph/0802.1532]. https://doi.org/10.1111/j.1365-2966.2008.13090.x.